

Development of Strain-Tunable Bilayer Graphene Devices

CNF Project Number: 2790-19

Principal Investigator(s): Katja C. Nowack

User(s): Brian T. Schaefer, Justin Oh

Affiliation(s): Laboratory of Atomic and Solid-State Physics, Department of Physics; Cornell University

Primary Source(s) of Research Funding: Cornell Center for Materials Research with funding from the NSF MRSEC program (DMR-1719875), National Science Foundation Graduate Research Fellowship under Grant No. DGE-1650441

Contact: kcn34@cornell.edu, bts72@cornell.edu

Website: <http://nowack.lassp.cornell.edu/>

Primary CNF Tools Used: Zeiss Supra SEM/Nabity, Trion Minilock III ICP etcher, 5x stepper

Abstract:

The direct application of uniaxial strain is a versatile and low-disorder technique to tune the electronic properties of materials [1]. Specifically, in two-dimensional materials with a hexagonal lattice, strain can result in a net magnetization with a purely orbital origin [2]. Dual-gated bilayer graphene is a versatile platform for studying this magnetization because the electronic bandgap and charge carrier density can be tuned widely and independently [3]. Here, we describe our efforts towards fabricating strainable multi-terminal bilayer graphene devices on flexible polyimide substrates. We continuously apply strain up to $\sim 1.4\%$ confirmed using Raman spectroscopy.

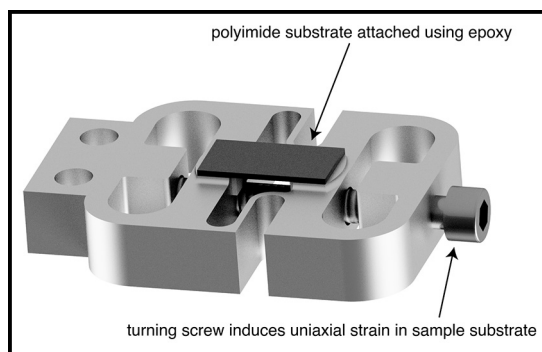


Figure 1: Custom titanium-based strain apparatus with polyimide substrate attached using Stycast 2850FT epoxy.

Summary of Research:

We use the custom titanium-based apparatus [4] illustrated in Figure 1 to apply strain to a polyimide substrate upon which our bilayer graphene devices are fabricated. Turning the screw displaces the two halves of the apparatus and enables continuous application of uniaxial tensile strain to a sample mounted to the split central platform. The maximum strain depends on the elastic modulus and geometry of the sample along with the yield strength of the epoxy used to attach the sample. Optical images of lithographically defined features on the surface of the substrate suggest a typical maximum strain of $\sim 2\%$ for polyimide substrates limited by failure of the epoxy.

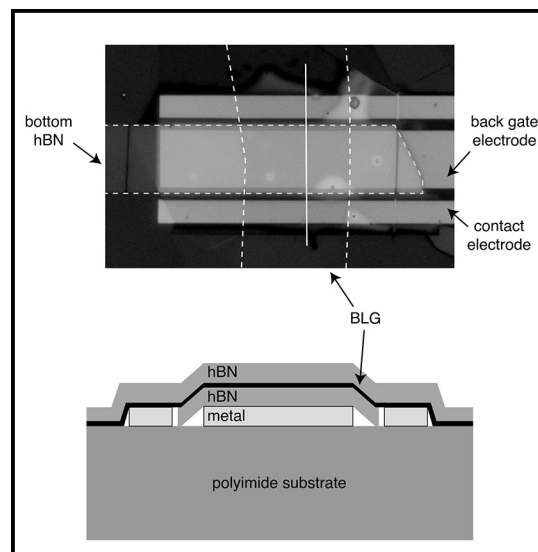


Figure 2: Top: optical image of a bilayer graphene device fabricated upon a polyimide substrate. Bottom: cross-sectional schematic along the solid line in the optical image.

Figure 2 shows an optical image and cross-sectional schematic of a strainable bilayer graphene device. We initially pattern metal electrodes for the device back gate and contacts onto a bare polyimide substrate. Next, we use a polymer-stamp-based dry-transfer technique [5] to sequentially pick up and transfer exfoliated flakes of bilayer graphene (BLG) and hexagonal boron nitride (hBN) onto the pre-patterned metal features.

We first transfer a single hBN flake onto the patterned electrodes and use reactive-ion etching (Trion Minilock III ICP Etcher) to uncover the metal contact electrodes. On top of this, we transfer a stack of hBN/BLG to complete the device. The top hBN flake facilitates the transfer of BLG, while the bottom hBN flake is a dielectric for the back gate. Encapsulation with hBN on both top and bottom improves the electronic quality of graphene devices [5]. Previous iterations of the fabrication process suggest that the direct areal contact between the BLG flake and polyimide substrate in our current design is essential for effective strain transfer from the substrate to the BLG flake.

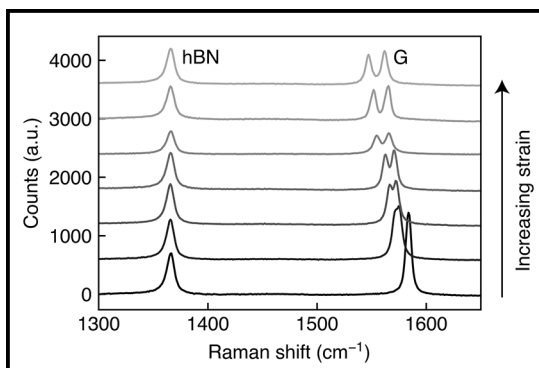


Figure 3: Strain evolution of the in-plane Raman peaks for BLG (labeled “G”) and hBN.

We use Raman spectroscopy to monitor changes in the vibrational modes of the lattice under application of strain, and use the position of the BLG “G” peak to estimate the amount of strain transfer. Figure 3 shows the evolution of the in-plane Raman peaks for hBN (“hBN”, $\sim 1366 \text{ cm}^{-1}$ at zero strain) and BLG (“G”, $\sim 1583 \text{ cm}^{-1}$ at zero strain) upon straining the substrate. The G peak shifts to lower wavenumber and splits into two distinct peaks, as expected for a hexagonal lattice with rotational symmetry broken by in-plane uniaxial strain [6]. The hBN peak is also expected to shift under uniaxial

strain, so the unchanging peak position suggests that strain is not transferred to hBN. The hBN-graphene interface exhibits notably low friction [7], so the lack of strain in the hBN layer is not surprising. Comparing the peak positions to those reported in the literature [6], we estimate that we induced at most $\sim 1.4\%$ uniaxial strain into this BLG device.

Conclusions and Future Steps:

We demonstrate application of uniaxial strain in a two-terminal bilayer graphene device fabricated on a metallic back gate and polyimide substrate. Moving forward, we aim to add a top gate electrode and identify improvements to the process that increase the yield of devices that strain reliably. This motivates investigation of the mechanism of strain transfer from the substrate into BLG. We then will study the effects of strain on the magnetic properties of our devices and extend this technique to other two-dimensional material systems.

References:

- [1] Wang, L. et al. Mobility Enhancement in Graphene by *in situ* Reduction of Random Strain Fluctuations. *Phys. Rev. Lett.* 124, 157701 (2020).
- [2] Lee, J., Wang, Z., Xie, H., Mak, K. F., and Shan, J. Valley magnetoelectricity in single-layer MoS_2 . *Nat. Mater.* 16, 887-891 (2017).
- [3] Zhang, Y., et al. Direct observation of a widely tunable bandgap in bilayer graphene. *Nature* 459, 820-823 (2009).
- [4] Sunko, V., et al. Direct Observation of a Uniaxial Stress-driven Lifshitz Transition in Sr_2RuO_4 . *npj Quantum Materials* 4 (2019).
- [5] Wang, L., et al. One-dimensional electrical contact to a two-dimensional material. *Science* 342, 614-617 (2013).
- [6] Tsoukleri, G., Parthenios, J., Galiotis, C., and Papagelis, K. Embedded trilayer graphene flakes under tensile and compressive loading. *2D Mater.* 2, 024009 (2015).
- [7] Song, Y., et al. Robust microscale superlubricity in graphite/hexagonal boron nitride layered heterojunctions. *Nat. Mater.* 17, 894-899 (2018).